Photoelectron and Auger-electron angular distributions of fixed-in-space CO_2

F. P. Sturm,[1,2,*] M. Schöffler,[1,2] S. Lee,[2] T. Osipov,[2] N. Neumann,[1] H.-K. Kim,[1] S. Kirschner,[1] B. Rudek,[1,2] J. B. Williams,[3] J. D. Daughhetee,[3] C. L. Cocke,[4] K. Ueda,[5] A. L. Landers,[3] Th. Weber,[2] M. H. Prior,[2] A. Belkacem,[2] and R. Dörner[1]

[1]*Institut für Kernphysik, Universität Frankfurt, Max-von-Laue Str. 1, D-60438 Frankfurt, Germany*

[2]*Chemical Sciences Division, Lawrence Berkeley National Laboratory, Berkeley, California 94720, USA*

[3]*Department of Physics, Auburn University, Auburn, Alabama 36849, USA*

[4]*Department of Physics, Kansas State University, Cardwell Hall, Manhattan, Kansas 66506, USA*

[5]*Institute of Multidisciplinary Research for Advanced Materials, Tohoku University, Sendai 980-8577, Japan*

(Received 4 June 2009; published 10 September 2009)

We report a kinematically complete experiment of carbon 1*s* photoionization of CO_2 including Auger decay and fragmentation. By measuring in coincidence of CO_2 C(1*s*) photoelectrons and ion fragments using synchrotron light at several energies above the C(1*s*) threshold, we determine photoelectron angular distributions as well as Auger-electron angular distributions with full solid angle in the molecular fixed frame. We confirm recent unexpected results showing an asymmetry of the photoelectron angular distribution along the molecular axis after ionization of the C(1*s*) orbital. Our high statistics and high resolution measurement unveils asymmetric features in the photoelectron angular distribution which change as a function of the kinetic energy release. This finding provides strong evidence that varying C–O bondlengths are the main cause for these asymmetries. The Auger-electron angular distributions do not show strong correlation with the photoelectrons.

DOI: 10.1103/PhysRevA.80.032506 PACS number(s): 33.60.+q, 33.80.Eh

I. INTRODUCTION

Recently Liu *et al.* [1] measured C(1*s*) photoelectron angular distributions in the molecular frame (MFPAD) of CO_2. They found an asymmetry of the MFPAD with respect to the O^+ and CO^+ fragments. The effect only appeared at 312 eV photon energy, where a shape resonance is located, and at 320 eV, giving rise to the assumption that resonance enhancements play a role in causing the asymmetry.

This observation is surprising for at least two reasons. First, the carbon dioxide molecule is linear with the carbon atom placed between the oxygen atoms. In the ground state the bond length between the carbon and both oxygen atoms is equal, around 2.2 bohr [2]. The C(1*s*) orbital is almost spherical-symmetrical and diffraction of the electron wave at the oxygen atoms at equal distance should produce a symmetric electron angular distribution with respect to the center of mass.

Second, Liu *et al.* argued that the observed asymmetry provides evidence for a breakdown of the well established two-step model. Here, the process of photoionization with subsequent Auger decay is regarded as two independent steps [3–5]. First the core electron is ejected from the molecule leaving it in an excited state. In a second step the core hole is filled by a valence electron, and another electron from an outer shell is ejected, usually carrying higher energy than the photo electron. Being doubly charged, the molecule dissociates via coulomb explosion. In the theoretical description this corresponds to a complete factorization of the transition into excitation and decay matrix elements without crossing or interference terms. This model would not hold if there is a mixing of the intermediate states, as this would mean that the knowledge of the intermediate state does not define the final Auger state and we could not regard them as independent any more.

As a possible explanation for the observed asymmetry, Liu *et al.* speculated that different C–O bond lengths of the individual molecule at the instant of photoabsorption could cause such an effect. In the vibrational ground state, the nuclear wave function is symmetric. However the measurement of a single photoionization event can find the molecule at asymmetric bond length. In such a case, the symmetry is broken by different C–O bond lengths on each side, and subsequent Auger decay makes it more likely for the longer bond to break. The photoelectron MFPAD itself will be asymmetric, since the photoelectron wave is multiply scattered in an asymmetric potential. Liu *et al.* presented calculations for different bond lengths which produce similar asymmetries. This speculative interpretation was confirmed by more elaborate theoretical work by Miyabe *et al.* [2], also considering the potential energy surfaces on which the asymmetric fragmentation proceeds. Nevertheless, independent experimental evidence for the proposed scenario was missing.

In the present paper we do not only confirm the asymmetry observed by Liu *et al.*, but in addition we provide direct experimental evidence for the proposed mechanisms by relating the MPFAD to the measured kinetic energy release (KER) of the fragments. Different internuclear distances at the instant of Auger decay lead to different KER. As a consequence, the asymmetry should vary with the KER, which is exactly what we observe. Furthermore we report the Auger-electron angular distribution in the molecular-fixed frame, which also shows a weak asymmetry.

II. EXPERIMENT

The experiment was performed at the EPU5 undulator beamline 11.0.2 of the Advanced Light Source synchrotron

*sturm@atom.uni-frankfurt.de; http://www.atom.uni-frankfurt.de

in Berkeley, CA. We used the well-established COLTRIMS technique [6] with a setup similar to the one used by Schöffler *et al.* [7] for measuring electron angular distributions in the molecular-fixed frame (see [8]). A supersonic gas jet of CO_2 at room temperature and at low driving pressure of about 1 bar crossed the photon beam at 90° angle in the vacuum chamber. Perpendicular to both axes a static electric field of 15 V/cm and a magnetic field of about 8.5 Gauss[1] guided the photoelectron and the ions to detectors on both sides of the spectrometer. Multichannel plates with delay-line anodes [9] provided time and position sensitive measurement. The photoelectrons were measured with 4π solid angle, whereas we narrowed the recoil ion acceptance angle to 21° to the spectrometer axis in order to gain sufficient resolution. In addition, we used an electrostatic lens to eliminate the degrading influence of the spatial target extension on the momentum resolution (see Fig. 12 in [10]). Configuration and functionality of the lens will be discussed in a separate publication. The resulting very high momentum resolution of the ionic fragments allowed us to use momentum conservation for calculating the full Auger-electron momentum vector. The molecular orientation in the laboratory frame at the instant of electron emission is given by the recoil ion dissociation axis, as the breakup of the double charged ion occurs on a fs time scale, much faster than molecular rotation (Axial recoil approximation). We measured at photon energies of 303, 312, 318.5, 319.5, 320.5, 321.5, and 322.5 ± 0.2 eV with horizontally polarized light and at 312 eV with circularly polarized light. The resolution of the angular distribution in the molecular frame depends on the orientation of the electron vector in the laboratory. For the photoelectrons produced at 312 eV photon energy, the uncertainty of the angle is ±5°, ±11°, and ±9°, for emission toward, perpendicular and away of the detector. We estimate a resolution of the Auger electrons of ±2.5° parallel to the detector and ±22.5° in the detector direction.

III. RESULTS AND DISCUSSION

A. Photoelectron MFPADs

Our measured photoelectron MFPADs for linear polarized light at several energies between $h\nu = 303$ and 322.5 eV and for circular polarization at 312 eV are shown in Fig. 1. These results are in excellent agreement with previous experiments [1,11], and data are within the error bars of these earlier measurements. At the shape resonance at 312 and at 320.5 eV photon energy, we confirm the asymmetry effect reported by Liu *et al.* At 312 eV, the photoelectron angular distribution shows higher intensity in the direction where the CO^+ ion flies after dissociation, whereas at 320 eV, the intensity is higher in the opposite direction. We should recall at this point, that the asymmetric breakup into a CO^+ ion and an O^+ ion occurs after emission of the photoelectron and the Auger electron. Hence, the observed asymmetry shows a definite link between the initial ionization step and the final bond breakage which survives the intermediate Auger decay. Below the shape resonance, we do not observe an asymmetry.

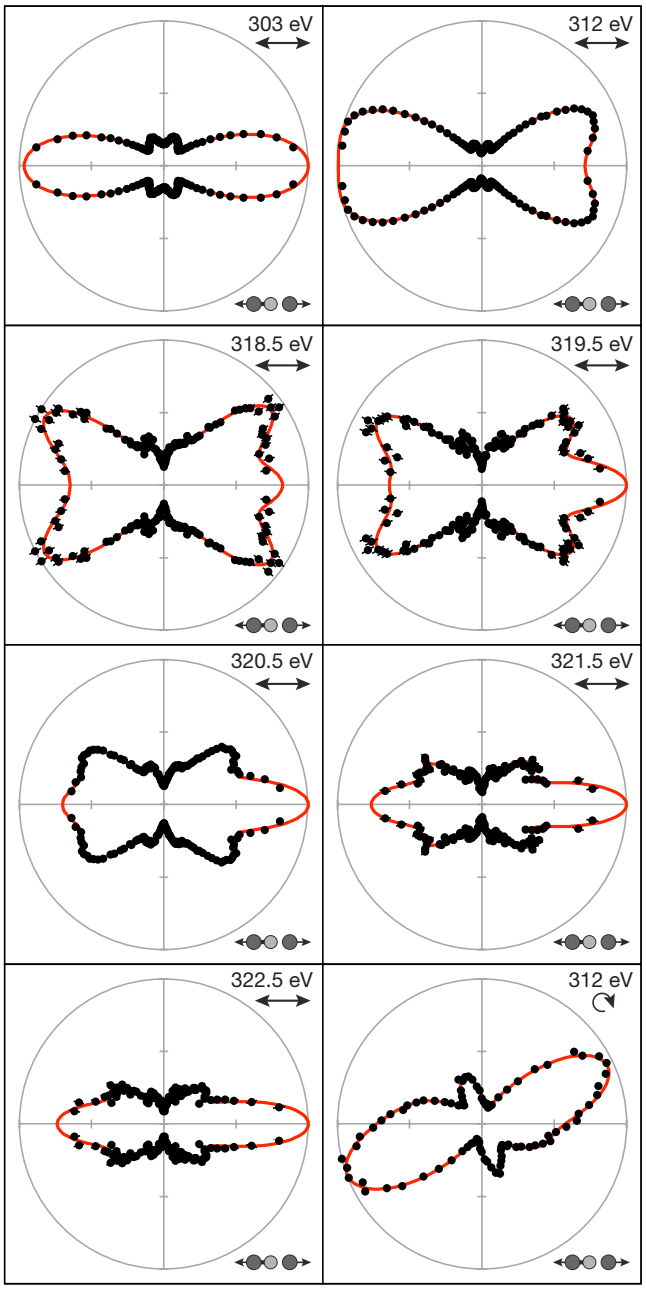

FIG. 1. (Color online) MFPADs at several energies above the carbon *K*-shell threshold with horizontal polarization and at 312 eV with circularly polarized light. The molecular axis is horizontal in the plots with the CO^+ ion pointing to the left. The angular distribution at 312 eV, shows a higher intensity for emission toward the CO^+ ion. At 320.5 eV, the emission is higher in the opposite direction. At circular polarization, the effect is weaker due to a higher contribution of the Π-transition perpendicular to the molecular axis. The solid lines are fits of the data with spherical harmonics up to l=5.

At low energies, *p*-wave contribution dominates clearly showing strong peaks along the molecular axis. Nevertheless, we were able to separate small contributions from higher order angular momenta, producing small peaks around perpendicular orientation to the molecular axis,

[1]Gauss for photon energies above 312 eV.

which were not resolved in the previous works. In the following, we show that these additional lobes allow us to unveil the mechanism producing the asymmetry. At higher energies, additional partial waves cause more complex distributions.

For circularly polarized light at 312 eV, the asymmetry is much reduced as compared to linear polarization. This is also consistent with the results from Liu *et al.*, since the transition matrix element for circular light is a coherent superposition of those for linear light parallel (Σ) and perpendicular (Π) to the molecular axis. The asymmetry is only visible in the Σ channel and is therefore much reduced for circular light.

In the following, we discuss three alternatives as a possible cause for the asymmetric angular distribution as suggested by Liu *et al.*: postcollision interaction, initial state correlation and bond length asymmetry. Since in our experiment in addition to the photoelectron, the Auger electron and the KER are measured in coincidence, we can test these hypotheses directly.

Post collision interaction describes the coupling of the fast Auger electron to the much slower photoelectron in the final state. In the present case, one could imagine that Auger decay from a valence orbital breaks the initial symmetry and leads to a preferred breakup of the bond from which the electron was ejected. If the Auger electron interacts with the photoelectron after emission, the originally symmetric photoelectron angular distribution would be modified and inherit some of the asymmetry of the Auger emission. In a recent work on neon 1*s* photoionization followed by Auger decay [12], it has been shown that PCI can play an important role at low photoelectron energies. We can check the influence of this mechanism directly by inspecting our MFPADs for different Auger-electron emission directions. If the asymmetry in the MFPAD were due to the imprint of asymmetric Auger decay, it should disappear for Auger emission perpendicular to the molecular axis, as in this case both directions along the molecular axis are affected equally. The blue dashed line in Fig. 2(a) shows our data for this geometry where PCI effects should not cause an asymmetry. Clearly, the asymmetry is still present, showing that another mechanism than PCI is responsible for the symmetry breaking. The inset in Fig. 2(b) reveals that the PCI, however, influences the relative emission distribution of photo- and Auger electrons. The ringlike distribution shows the emission intensity at all angles between photo- and Auger electron. There is a small but significant suppression of flux for both electrons emitted in the same direction (see [12]). This suppression of flux for parallel emission does influence the MFPAD also when the Auger electron is selected parallel or antiparallel to the CO^+-O^+ axis as shown by the red and green line in Fig. 2(a) [compare curves at $\cos(\theta)=1$].

We now discuss initial state correlation as a possible cause of the asymmetry. This model is based on the assumption that the single orbital picture is incomplete, neglecting an important part of electron correlation. In the two-step model as introduced above, one considers the photoejection from the C(1*s*) orbital and independent of that subsequent relaxation. This happens via Auger transition again between well defined molecular orbitals. In the bound state, molecular orbitals can be mixed through electron correlation. Electron

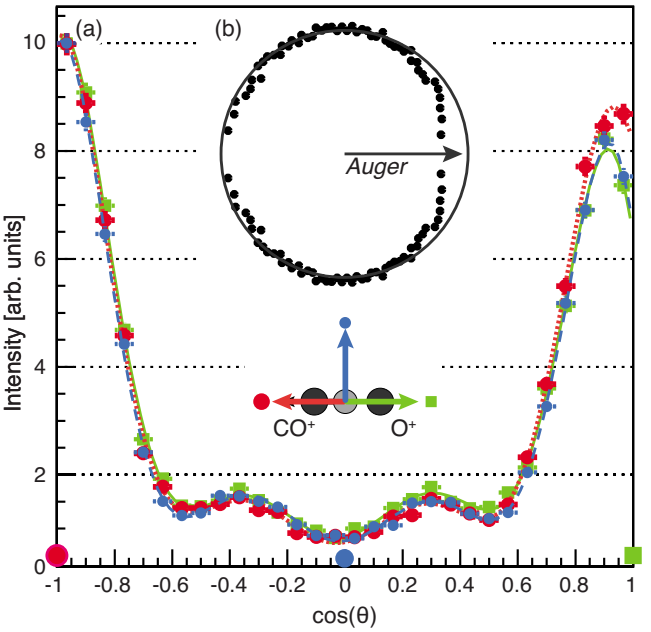

FIG. 2. (Color online) MFPADs for fixed Auger ejection angles (γ=312 eV, horiz. polariz., normalized to the maximum): red dotted line, big dots—Auger emission toward CO^+; green line, squares—Auger emission toward O^+; blue dashed line, small dots—Auger emission perpendicular to the molecular axis. The blue distribution proves that PCI does not cause the asymmetry along the molecular axis. The inset shows a polar plot of the photoelectron intensity for varying angle between photoelectron and Auger electron. The arrow represents the direction of the Auger electron, which is fixed in this plot to the right.

correlation might also couple photo- and Auger electron similarly as PCI does via electron-electron interaction in the continuum state. With our experiment, we are able to look at dependencies between photoelectrons and Auger electrons. Our data did not provide any evidence for important correlation or dependency of photoelectrons and Auger electrons, as observed in N_2 [7], beyond what is shown in Fig. 2. This is also expected, since the energy difference between the involved orbitals is rather large. For small energy spacings, like the g/u splitting of N_2 or Ne_2 such couplings are strong and lead to spectacular changes of the MFPAD as a function of the Auger emission angle [7,13,14]. Similarly, intermediate resonances have been reported to lead to large asymmetries [15]. In the present case of CO_2, there are no such resonances involved.

The third possibility of causing an asymmetric MFPAD is an asymmetry in the molecular geometry at the instant of photoelectron ejection, as outlined in the introduction. On average, carbon dioxide is a linear molecule, and both C–O bonds have the same length. However, asymmetric stretching of the molecular bonds provides a distribution of bond lengths in which only the peak represents a symmetric molecule. In cases when the ejection of the photoelectron occurs at nonequal C–O bond length, the interference pattern of the electron wave diffracted in the asymmetric molecular potential will be asymmetric. Since the Auger decay is on the same time scale (Auger lifetime: ~6 fs [16]) as the asymmetric stretch motion (quarter period 3.55 fs [2]), the asym-

metric bond length at the instant of photoabsorption could finally lead to a preferred side for the bond breakage after Auger emission. Our approach to demonstrate molecular distances as the result of asymmetric MFPADs is to look for differences in the MFPAD as a function of the KER. The kinetic energy release is the sum of the kinetic energies of all ions after breakup due to the Coulombic potential between the charged ions. Its distribution reflects the transition of the core-hole state to the final state and depends on the internuclear distance at breakup time. In this sense, the KER can be used as a measure of the internuclear distance. We have to consider that several repulsive final states are populated, and the measured KER distribution is always a mixture of the different final state distributions. Different KERs can therefore be due to different internuclear distances and dissociation along different CO_2^{2+} potential energy surfaces.

The measurement of internuclear distance by detecting the KER is based on the reflection approximation (see, e.g., [17]). It has been pioneered in coulomb explosion imaging in ion beams [18] and is routinely used with strong laser fields today (see, e.g., [19]). We apply this idea here to measure the internuclear distance for each single event with a precision much better than the width of the ground-state nuclear wave function. Our coincident detection of KER and electron momentum allows us to select, from the ground-state wave function, a subsample of molecules which had a particular internuclear distance at the instant of the electronic transition. We have demonstrated this technique previously for coherent Rutherford scattering [20]. For photodoubleionization of H_2 with the same technique, it has been shown that correlated electron emission [21] and electron defraction [22–24] depends on the internuclear distance.

In our data we find a small but significant dependence of the asymmetry with respect to the KER. For rising KER, we observe a decrease in the asymmetry for the emission along the molecular axis from 20% to about 10% [solid line in Fig. 3(e)]. The small *f*-wave lobes exhibit slightly more pronounced changes. If we look at these two peaks around perpendicular emission to the molecular axis, intensity is higher for photoelectron emission at negative $\cos(\theta)$ for KER values below 9 eV, whereas the peak at positive $\cos(\theta)$ becomes higher above this value. In Fig. 3 one can see details for several KER values (b)–(d) as well as a graph covering the complete range (f). In the theoretical model calculated by Miyabe *et al.* [2], such a shift for different bond lengths is predicted as well, and we conclude that asymmetries in the initial geometry of the molecule are the likely source of the observed asymmetric MFPAD.

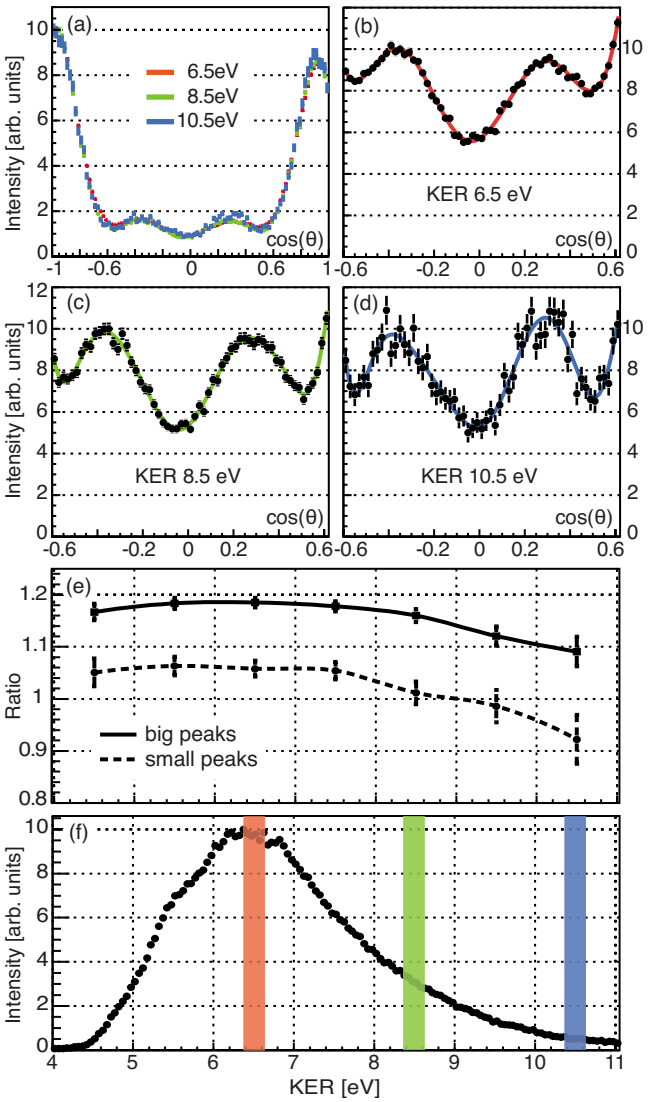

FIG. 3. (Color online) MFPADs for different kinetic energy releases (KER)(γ=312 eV, hor. polariz.). The cosine of the angle to the molecular axis is plotted. Positive values correspond to the direction of the O^+. In panel (a) we can see only small changes in the MFPAD for different KERs. However, a closer inspection of the small lobes from *f*-wave contributions (b), (c), and (d) reveals a swapping of the asymmetry from the CO^+ to the O^+ side at higher KER. (e) shows the ratio of the maximum of left to right peak as a function of KER. The solid curve represents the ratio of the main peaks, the dotted line the small features at $\cos(\theta) = \pm 0.35$, illustrating the evolution of the asymmetry with the molecular bond length. (f) shows the KER spectrum, regions chosen for the data in (b), (c), and (d) are marked in the particular color.

B. Auger-electron angular distributions

We present here Auger-electron angular distributions of fixed-in-space CO_2. Such angular distributions are known to be a rich source of information on the states involved as well as on the molecular potential from which the Auger electrons escape. The shape of the initial and final state orbital is imprinted onto the Auger angular distribution [25–27]. As a consequence, the angular distributions for Σ and Π transitions are preferentially along or perpendicular to the bond, respectively. In addition, the multiple scattering of the Auger electron in the molecular potential leads to interference effects in the angular distributions of the Auger electron [5,25].

Therefore, one might expect that an asymmetry would be present in the Auger angular distribution, such as the one seen in the MFPAD. Since the bond breakage is directly associated with the emission of the Auger electron, any correlation of its angular distribution with the site at which the

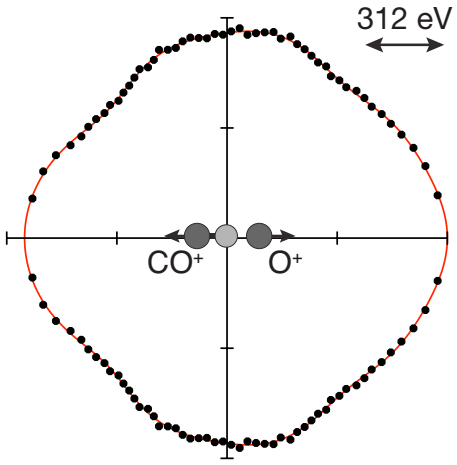

FIG. 4. (Color online) Auger-electron angular distributions for at 312 eV photon energy with horizontal polarization.

C–O bond breaks can be expected to be even stronger than for the photoelectron.

Nevertheless, our measured angular distributions shown in Fig. 5 display only a rather weak asymmetry. The angular distribution in general is close to isotropic (see Fig. 4). Our data do not exhibit dependence of this small asymmetry on the photon energy. They rather indicate that it is the shape resonance which enhances the asymmetry effect, and for photo- and Auger electrons with energies much above the shape resonance, the asymmetries are rather small.

The Auger-electron angular distribution contains contributions from Σ and Π states. The mixing of these states changes however with the KER, as seen in Fig. 5. At low kinetic energy releases, the distribution is almost isotropic with equal intensity of Auger-electron emission along and perpendicular to the molecular axis. At KER values of 6–9 eV, a weak asymmetry along the molecular axis can be observed which is likely to reflect the effect observed in the MFPADs. Above KER=6 eV, there are rising contributions from higher order angular momentum, yielding small lobes around $\cos(\theta) = \pm 0.35$ as seen in the MFPAD. At larger KER, the distribution exhibits significantly more intensity along the molecular axis, indicating a stronger contribution of Σ states.

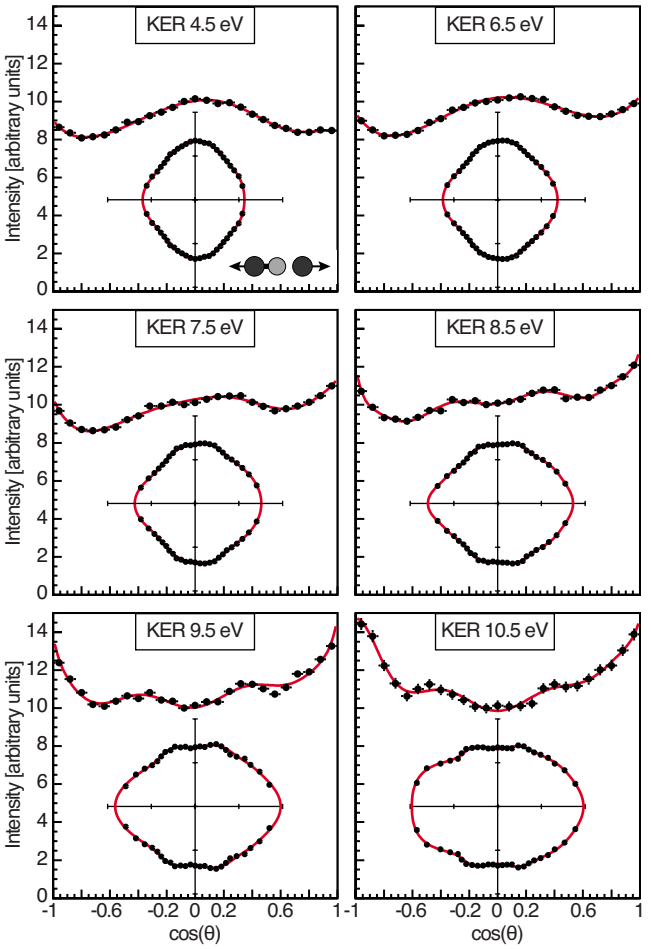

FIG. 5. (Color online) Auger-electron angular distributions for different KER at 312 eV photon energy with horizontal polarization. The insets show the distribution as a polar plot where the molecular axis is fixed horizontally. The distribution reflects the selection of Auger final states for different KER. At lower KER, mainly Π-states contribute whereas Σ-states gain more weight at higher KER, shifting intensity to Auger-electron emission along the molecular axis. Intensity is normalized to $\cos(\theta)=0$. The solid lines are fits by spherical harmonics up to $l=5$.

IV. SUMMARY

We have presented the first kinematically complete experiment on two-step double photoionization of CO_2 followed by fragmentation into $CO^+ + O^+$. The molecular-frame angular distribution of the photoelectron emitted from the central carbon 1*s* shell shows an asymmetry in the region of the shape resonance. By observing MFPADs at different kinetic energy releases, we provide direct experimental evidence that varying C–O bond lengths cause an asymmetry of the photoelectron angular distribution along the molecular axis. Our high resolution measurements reveal new details in the MFPADs produced by higher order angular momenta and presented CO_2 Auger-electron angular distributions in the molecular-fixed frame. Our data show clearly a link between photo and Auger electron (PCI) as well as a dependence of photo and Auger electron on the nuclear motion and on asymmetries in the dissociation. The level of detail of our study calls for a unified theoretical treatment of photoemission, Auger decay and nuclear motion.

ACKNOWLEDGMENTS

We thank X.-J. Liu for motivating this experiment. Special thanks to H. Bluhm, T. Tyliszczak, D. Kilcoyne, and the whole team of the ALS for great support. We profited from discussion with W. M. McCurdy and T. Rescigno. The work was supported by the Department of Energy, Office of Basic Energy Sciences, Chemical Sciences Division under Contract No. DE-AC02-05CH11231. Support by DAAD and DFG are gratefully acknowledged.

[1] X. Liu, H. Fukuzawa, T. Teranishi, A. De Fanis, M. Takahashi, H. Yoshida, A. Cassimi, A. Czasch, L. Schmidt, R. Dörner, K. Wang, B. Zimmermann, V. McKoy, I. Koyano, N. Saito, and K. Ueda, Phys. Rev. Lett. **101**, 083001 (2008).
[2] S. Miyabe, C. W. McCurdy, A. E. Orel, and T. N. Rescigno, Phys. Rev. A **79**, 053401 (2009).
[3] V. Kuznetsov and N. Cherepkov, J. Electron Spectrosc. Relat. Phenom. **79**, 437 (1996).
[4] R. Guillemin, E. Shigemasa, K. Le Guen, D. Ceolin, C. Miron, N. Leclercq, P. Morin, and M. Simon, Phys. Rev. Lett. **87**, 203001 (2001).
[5] T. Weber, M. Weckenbrock, M. Balser, L. Schmidt, O. Jagutzki, W. Arnold, O. Hohn, M. Schöffler, E. Arenholz, T. Young *et al.*, Phys. Rev. Lett. **90**, 153003 (2003).
[6] J. Ullrich, R. Moshammer, A. Dorn, R. Dörner, L. Schmidt, and H. Schmidt-Böcking, Rep. Prog. Phys. **66**, 1463 (2003).
[7] M. Schöffler, J. Titze, N. Petridis, T. Jahnke, K. Cole, L. Schmidt, A. Czasch, D. Akoury, O. Jagutzki, J. Williams *et al.*, Science **320**, 920 (2008).
[8] A. Landers, T. Weber, I. Ali, A. Cassimi, M. Hattass, O. Jagutzki, A. Nauert, T. Osipov, A. Staudte, M. H. Prior *et al.*, Phys. Rev. Lett. **87**, 013002 (2001).
[9] O. Jagutzki, V. Mergel, K. Ullmann-Pfleger, L. Spielberger, U. Spillmann, R. Dörner, and H. Schmidt-Böcking, Nucl. Instrum. Methods Phys. Res. A **477**, 244 (2002).
[10] R. Dörner, V. Mergel, O. Jagutzki, L. Spielberger, J. Ullrich, R. Moshammer, and H. Schmidt-Böcking, Phys. Rep. **330**, 95 (2000).
[11] N. Saito, A. De Fanis, K. Kubozuka, M. Machida, M. Takahashi, H. Yoshida, I. Suzuki, A. Cassimi, A. Czasch, L. Schmidt *et al.*, J. Phys. B **36**, L25 (2003).
[12] A. L. Landers, F. Robicheaux, T. Jahnke, M. Schöffler, T. Osipov, J. Titze, S. Y. Lee, H. Adaniya, M. Hertlein, P. Ranitovic *et al.*, Phys. Rev. Lett. **102**, 223001 (2009).
[13] K. Kreidi, T. Jahnke, T. Weber, T. Havermeier, R. Grisenti, X. Liu, Y. Morisita, S. Schössler, L. Schmidt, M. Schöffler *et al.*, J. Phys. B **41**, 101002 (2008).
[14] M. Yamazaki, J. I. Adachi, Y. Kimura, A. Yagishita, M. Stener, P. Decleva, N. Kosugi, H. Iwayama, K. Nagaya, and M. Yao, Phys. Rev. Lett. **101**, 043004 (2008).
[15] F. Martin, J. Fernandez, T. Havermeier, L. Foucar, T. Weber, K. Kreidi, M. Schöffler, L. Schmidt, T. Jahnke, O. Jagutzki *et al.*, Science **315**, 629 (2007).
[16] T. X. Carroll, J. Hahne, T. D. Thomas, L. J. Sæthre, N. Berrah, J. Bozek, and E. Kukk, Phys. Rev. A **61**, 042503 (2000).
[17] E. A. Gislason, J. Chem. Phys. **58**, 3702 (1973).
[18] Z. Vager, R. Naaman, and E. P. Kanter, Science **244**, 426 (1989).
[19] F. Legare, K. F. Lee, I. V. Litvinyuk, P. W. Dooley, S. S. Wesolowski, P. R. Bunker, P. Dombi, F. Krausz, A. D. Bandrauk, D. M. Villeneuve *et al.*, Phys. Rev. A **71**, 013415 (2005).
[20] L. P. H. Schmidt, S. Schössler, F. Afaneh, M. Schöffler, K. E. Stiebing, H. Schmidt-Böcking, and R. Dörner, Phys. Rev. Lett. **101**, 173202 (2008).
[21] T. Weber, A. O. Czasch, O. Jagutzki, A. K. Müller, V. Mergel, A. Kheifets, E. Rotenberg, G. Meigs, M. H. Prior, S. Daveau *et al.*, Nature (London) **431**, 437 (2004).
[22] K. Kreidi, D. Akoury, T. Jahnke, T. Weber, A. Staudte, M. Schöffler, N. Neumann, J. Titze, L. P. H. Schmidt, A. Czasch *et al.*, Phys. Rev. Lett. **100**, 133005 (2008).
[23] D. Akoury, K. Kreidi, T. Jahnke, T. Weber, A. Staudte, M. Schöffler, N. Neumann, J. Titze, L. P. H. Schmidt, A. Czasch *et al.*, Science **318**, 949 (2007)
[24] M. S. Schöffler, K. Kreidi, D. Akoury, T. Jahnke, A. Staudte, N. Neumann, J. Titze, L. P. H. Schmidt, A. Czasch, O. Jagutzki *et al.*, Phys. Rev. A **78**, 013414 (2008).
[25] K. Zähringer, H.-D. Meyer, and L. S. Cederbaum, Phys. Rev. A **46**, 5643 (1992).
[26] S. Bonhoff, K. Bonhoff, and K. Blum, J. Phys. B **32**, 1139 (1999).
[27] D. Rolles, G. Prümper, H. Fukuzawa, X.-J. Liu, Z. D. Pešić, R. F. Fink, A. N. Grum-Grzhimailo, I. Dumitriu, N. Berrah, and K. Ueda, Phys. Rev. Lett. **101**, 263002 (2008).